Received Date : 02-Jun-2016
Revised Date : 14-Oct-2016
Accepted Date : 14-Nov-2016
Article type : Original Article

The regulation of carotenoid formation in tomato fruit

Eugenia M.A. Enfissi, Marilise Nogueira, Peter M. Bramley, and Paul D. Fraser*

School of Biological Sciences, Royal Holloway, University of London, Egham, Surrey,

TW20 OEX, UK.

*Address correspondence to: p.fraser@rhul.ac.uk Tel. +44 (0)1784 443894

Additional author email addresses:

genny.enfissi@rhul.ac.uk

Marilise.Nogueira.2010@live.rhul.ac.uk

p.bramley@rhul.ac.uk

Running title: Regulation of β–carotene formation in tomato

Key words: Solanum lycopersicon, carotenoid, isoprenoid

SUMMARY

Carotenoid biosynthesis in plants includes a complex series of desaturation/isomerisation reactions, catalysed by four independent enzymes. In bacteria and fungi one desaturase/isomerase enzyme completes the same series of

This article has been accepted for publication and undergone full peer review but has not been through the copyediting, typesetting, pagination and proofreading process, which may lead to differences between this version and the Version of Record. Please cite this article as doi: 10.1111/tpj.13428

reactions. In the present study, a bacterial desaturase (*crtI*) from *Pantoea ananatis* has been overexpressed in the *tangerine* mutant of tomato (*Solanum lycopersicon*) which accumulates *cis* carotene isomers in the fruit due to a defective isomerase (CRTISO) and the *old gold crimson* (*og*^{c}) tomato mutant, which is defective in the fruit-enhanced lycopene β-cyclase (*CYCB*). Comprehensive molecular and biochemical characterisation of the resulting lines expressing *crtI* has revealed negative feedback mechanisms, acting predominantly at the level of phytoene synthase-1 (*PSY1*), and feed-forward mechanisms inducing cyclisation. In both cases, altered transcription appears to be the progenitor, with subsequent post-transcriptional modulation highlighting the complexity of the processes involved in modulating carotenoid homeostasis in plant tissues.

INTRODUCTION

Carotenoids represent the largest class of natural pigments found in nature. They are synthesised in all photosynthetic bacteria, some non-photosynthetic bacteria, fungi, algae and higher plants (Hirschberg, 2001; Fraser and Bramley, 2004). In plants, carotenoids perform a diverse array of roles, including acting as ancillary photosynthetic pigments, free radical scavengers (Demmig-Adams and Adams, 2002) and precursors of the phytohormone abscisic acid (Schwartz et al., 2003). Other carotenoid-derived products are believed to be signalling/regulators involved in plant development (Avendano-Vazquez et al., 2014).

Humans cannot synthesise carotenoids *de novo*; instead they must be acquired from the diet. The intake of fruit and vegetables rich in carotenoids has been shown, from epidemiological and intervention studies, to reduce the onset of chronic disease states, such as certain cancers, age-related macular degeneration and cardiovascular diseases (Fraser and Bramley, 2004;

Krinsky and Johnson, 2005). High dietary intake of lycopene, an acyclic carotenoid with potent antioxidant properties, has been implemented in the reduced incidence of certain cancers (Rao et al., 1999; Story et al., 2010). In the western diet, tomato (*Solanum lycopersicum*) is the principal source of lycopene and an important source of β-carotene (provitamin A), as well as other health promoting phytochemicals such as tocopherols, phenylpropanoids and flavonoids.

Carotenoids are isoprenoids and, thus, derived from the universal five carbon precursor isopentenyl pyrophosphate (IPP, C_5). In higher plants they are synthesised in the plastid using IPP generated from the methylerythritol-4-phosphate (MEP) pathway (Pulido et al., 2013). Geranylgeranyl pyrophosphate (GGPP, C_{20}) is the prenyl lipid precursor utilised to form carotenes. Two molecules of GGPP are condensed in a head-to-head manner by phytoene synthase (Fraser and Bramley, 2004). This reaction represents the first committed step in carotenoid formation. Phytoene undergoes a series of sequential desaturation (dehydrogenation) steps to yield lycopene via phytofluene, ζ-carotene and neurosporene. Carotene isomerisation from *cis* to *trans* geometric configurations is also an integral component of the sequence. These sequences of carotene desaturation/isomerisation reactions are complex and have attracted great interest over the last decade. In part, this is due to their existence as herbicide targets (Sandmann et al., 1990) and as key steps in the generation of "Golden Rice" (Ye et al., 2000). In order to arrive at our present understanding of carotene desaturation/isomerisation numerous genetic, inhibitor, *in vivo* complementation (Linden et al., 1991) and *in vitro* studies (Fraser et al., 1992; Fraser et al., 1993; Schaub et al., 2012) have been performed.

The consensus from several recent reports (Isaacson et al., 2004; Breitenbach and Sandmann, 2005; Yu et al., 2011; Gemmecker et al., 2015) suggests that the series of intermediates proceed from 15-*cis*-phytoene to 9,15,9'-*tri*-*cis*-ζ-carotene via 15,9'-*di*-*cis*-phytofluene (Figure 1). These reactions are catalysed by phytoene desaturase (PDS). 9,15,9'-*tri*-*cis*-ζ-Carotene is then converted to 9,9'-*di*-*cis*-ζ-carotene, via a non-enzymatic mechanism, presumably light and chlorophyll or the enzyme designated ZISO (Chen et al., 2010; Beltran et al., 2015). The 9,9'-*di*-*cis*-ζ-Carotene can then be desaturated by ζ-carotene desaturase (ZDS) to yield 7,9,9'-*tri*-*cis*-neurosporene, which accordingly is desaturated further to 7,9,7',9'-*tetra*-*cis*-lycopene (prolycopene, Figure 1). In contrast, the desaturation/isomerisation sequence deduced from characterisation of the tomato carotene isomerase is 7,9,9'-*tri*-*cis*-neurosporene isomerisation to 9'-*cis*-neurosporene by CRTISO, then desaturation by ZDS to 7',9'-*di*-*cis*-lycopene, which is further isomerised to all-*trans* lycopene by CRTISO (Yu et al., 2011). Although the *tangerine* mutant **(t^{3183})** possesses a defective isomerase, *cis* desaturation intermediates are not detectable in its photosynthetic tissues, as it is postulated that light and chlorophyll can overcome the action of the isomerase enzyme (Isaacson et al., 2002; Park et al., 2002). In bacteria and fungi, complementation studies with purified enzymes have shown that 15-*cis*-phytoene is converted to all-*trans*-lycopene, the isomerisation postulated at the level of phytoene (Fraser et al., 1992) or prolycopene (Schaub et al., 2012), Figure 1).

In the present article, a bacterial phytoene desaturase/isomerase, *crtI*, from *Pantoea ananatis* (formally *Erwinia uredovora*) has been expressed in (i), the *tangerine* (t^{3183}) mutant of tomato, which has a defective allele in the *CRTISO* gene and thus, carotenes in the *cis* configuration predominate and (ii), the *old gold crimson* (og^{c}) mutant which has a null mutation in the chromoplast-specific lycopene cyclase, *CYCB*, resulting in lycopene

accumulation (Ronen et al., 2000). Characterisation of the transformants has identified important ~~new~~ regulatory mechanisms that operate within and beyond the carotenoid pathway *in vivo*.

RESULTS

Transgenic *tangerine* tomato plants expressing a bacterial carotene desaturase/isomerase (*crtI*) accumulate β-carotene

Of the eleven primary transgenic lines of *tangerine* (t^{3183}) tomato plants expressing the bacterial *crtI*, nine contained single inserts and two, multiple inserts. In addition to kanamycin resistance, the presence of *crtI* in each line was confirmed by PCR. These *tangerine* lines containing *crtI* were designated *t*:*crtI*-1 to 11 and compared to their control t^{3183} allele in the Ailsa Craig (AC) background, as well as AC itself (wild type) and previously generated AC lines expressing *crtI*; AC:*crtI*, (Romer et al., 2000). Phenotypically, vegetative tissues from the *t*:*crtI* lines appeared similar to the *tangerine* and AC varieties, apart from paler pigmentation in very young leaves. This observation was also previously found with the AC:*crtI* transgenic lines (Romer et al., 2000). Pigment analysis of the leaf and mature green fruit tissue confirmed that they contained lower levels of chlorophyll and carotenoids in comparison to their parental lines (Table 1A, B). With the onset of ripening, a colour change was evident. A dark orange colouration was observed in *t*:*crtI* fruit, compared to the yellow/orange colour of the t^{3183} mutant fruit (Figure S1) or the characteristic red colour of AC fruit and red/orange of the AC:*crtI* genotype (Romer et al., 2000).

Analysis of ripe fruit from the t^{3183} and *t*:*crtI* lines showed a clear change in carotenoid content. Identification and quantitation of carotenoids, including that of the *cis* and *trans* isomers, was verified by a combination of HPLC (system II), TLC, spectral characteristics and mass spectrometry (Table S1 and Figure S2). The most striking feature

was the presence of β-carotene in *t*:*crtI* and its absence in t^{3183} in both primary and subsequent generation transformants. The carotenoid profile of ripe fruit of t^{3183} was an accumulation of phytoene and phytofluene, between 26-50% of the total carotenoid content. Phytoene was present as the 15-*cis* geometric isomer, with the all-*trans* isomer only comprising 5% of the total phytoene. All-*trans* and *cis*-lycopene geometric isomers were detectable at low levels (<14μg/g DW), whilst prolycopene accumulated to high levels (1-2 mg/g DW) and β-carotene was absent in the ripe fruit. Low levels of lutein (<10μg/g DW) were also detected in t^{3183} (Table 1C and Table S2). In all *t*:*crtI* primary lines phytoene and phytofluene levels were reduced between 40-80% and 35-75%, respectively (Table S2). The presence of prolycopene was reduced by between 35-78% in most cases. Lutein levels were increased 2.7 to 5.8-fold. Lycopene and β-carotene were detected in the all-*trans* forms in a unique manner compared to the t^{3183} background (Table S2). Concurrent analysis with AC and AC:*crtI* lines established a similar trend, with the phytoene and phytofluene levels reduced in the presence of *crtI*. The level of all-*trans*-lycopene was also reduced similarly to the reduction in prolycopene observed in *t*:*crtI* lines. β-Carotene levels were increased (~3.5-fold) in the AC:*crtI* and lutein levels were also elevated, as in the *t*:*crtI* lines (Table S2). From four primary events possessing single inserts for the transgene, a T_1 population was generated. Zygosity was determined by Southern blotting and the presence of the crtI protein demonstrated by Western blotting. The stability of the chemotype was then subsequently assessed over a further two generations. As described earlier, the overriding feature of the carotenoid profile found in the ripe fruit of the *t*:*crtI* events was the presence of β-carotene and all-*trans* lycopene, both of which are absent in the *tangerine* background and the azygous lines analysed in the T1 generation (Table S3). Although present in the *t*:*crtI* lines, all-*trans* lycopene only represented 6% of the AC lycopene content in stable homozygous lines (T2 generation; Table 1C). However, the level of β-carotene present in the *t*:*crtI* lines exceeded

3.8-fold that found in the AC. Phytoene and all derived desaturase intermediates were reduced in the *t*:*crtI* lines compared to both the t^{3183} background and AC (Table 1C). For example, phytoene and phytofluene were reduced 3-fold and 7-fold respectively compared to AC and 12-fold and 11-fold respectively compared to *tangerine*. *cis*-ζ-Carotene was reduced 2-fold compared to AC and 9-fold compared to t^{3183}. *cis*-Neurosporene was absent in the *t*:*crtI*, compared to its tangerine background. In effect, the *t*:*crtI* profile of desaturase intermediates resembled that found in the AC background. The chemotype of the *t*:*crtI* lines was consistent in the homozygous state and stable in subsequent generations. The profile of carotenoids was similar to that of the AC:*crtI* plants, where β-carotene was increased, whilst intermediates such as phytoene and phytofluene decreased.

crtI Transgenic lines have altered levels of transcripts responsible for carotenoid biosynthesis

Transcripts from stable *t*:*crtI* transformants are displayed relative to the Ailsa Craig wild type background in Figure 2. It is apparent that changes in the expression of biosynthetic genes throughout the pathway resulted from the effects of *crtI* expression. One of the most notable responses was that of the specific cyclase genes, which were also dependent on the parental background. In AC:*crtI*, the *LCYB* chloroplast gene was upregulated and the expression of the *CYCB* ripening specific cyclase remained unchanged. However, in *t*:*crtI* lines *CYCB* expression was doubled compared to *tangerine*, whilst the expression of the *LCYB* gene was not affected. In both AC:*crtI* and *t*:*crtI* lines, expression of the epsilon cyclase was also significantly increased compared to their respective backgrounds (~8-fold; Figure 2 and Table S4). However, this increase in expression did not result in an equivalent increase in lutein in either case, (in *t*:*crtI* lutein increased 1.5-fold; no change in AC:*crtI*), (Table 1C). Conversely, an overall reduction in the level of phytoene synthase expression

was observed in both AC:*crtI* and *t*:*crtI* lines. The expression profiles of *PSY*2 were very similar in both AC and *tangerine* fruit and subsequently in the *crtI* expressing lines, where it was down-regulated in both backgrounds. The expression of *PDS* was upregulated in t^{3183} fruit compared to AC, presumably in response to the high levels of phytoene that accumulate in these fruit. The presence of the bacterial desaturase in this background resulted in the further up-regulation of *PDS*. Its presence also up-regulated *PDS* in the AC background. The expression of *CRTISO* in AC:*crtI* was very similar to that of *PDS*, showing a ~2-fold increase. However, as expected, its expression in *tangerine* lines was barely detectable, at 0.008-fold that of the AC level. Other genes found to be altered in their expression level in response to the presence of *crtI* were geranylgeranyl pyrophosphate reductase (*GGDPR*) and γ-tocopherol methyltransferase (*GTMT*). Both genes were found to be significantly up-regulated (*GGDPR* 5 - 10 fold and *GTMT* ~1.6 fold) in both backgrounds (Figure S3A). This corresponded with a 2-fold increase in α-tocopherol, whilst γ-tocopherol was undetectable in *crtI* expressing lines (Figure S3B).

Isoprenoid enzyme activities are altered in the transgenic fruit

Although practically demanding, *in vitro* enzyme activities were determined throughout the pathway (Table3), in order to add an additional layer cellular regulation to the study. DXS activity was 1.5-fold higher in t^{3183} compared to AC extracts. The effect of crtI on DXS activity was similar in both the AC:*crtI* and *t*:*crtI*, with an approximate 2-fold reduction in activity. In a similar manner, the effect of crtI on IPP isomerase was a 2-fold reduction in both AC:*crtI* and *t*:*crtI*. However, in this instance, no difference in IPP isomerase activity was observed between the AC and t^{3183} genotypes. GGPPS activity in the *tangerine* extracts was almost 2-fold greater than that found in AC. In the AC background, crtI had no effect on GGPPS activity. However, in the t^{3183} background, the presence of crtI resulted in a

~2-fold reduction in activity. The effect of crtI in both the t^{3183} and AC backgrounds was a reduction in phytoene synthase activity, but the reduction was more pronounced in the *t*:*crtI* extracts. In addition to specific *in vitro* assays, incorporation from the precursor ^{14}C-IPP was carried out (Figure S3C). Comparison between AC and t^{3183} extracts indicated that the latter incorporated IPP into GPP, FPP, GGPP and phytoene 2 to 4-fold greater, although phytol levels were similar. Thus, this trend was consistent with the *in vitro* assays from GGPPS and PSY (Table3). Extracts from AC:*crtI* displayed increased incorporation into GPP and FPP, but reduced incorporation into GGPP, phytol and phytoene. Determination of ^{14}C-IPP incorporation by *t*:*crtI* extracts compared to *tangerine* controls showed a reduced incorporation into GPP, FPP, GPP, phytol and phytoene (Figure S3C). These data for AC:*crtI* and *t*:*crtI* correlated with the levels of specific enzyme activities determined (Table3). Total *in vitro* phytoene desaturation in the t^{3183} membrane preparation was 2-fold less than that determined in the AC (Table3). When crtI was present in t^{3183}, total desaturation increased almost 2-fold. Analysis of individual products indicated the greatest increases in β-carotene (2 to 4-fold), with extracts from AC:*crtI* and *t*:*crtI* compared to AC and *tangerine*, respectively (Table S5). Prolycopene was reduced when crtI-containing extracts were used. Lycopene levels were not altered in AC:*crtI* relative to AC but increased in *t*:*crtI* relative to t^{3183}, as a result the *in vitro* profiles correlated with the steady state levels determined (Table S5 and Table 1C).

Significant changes in metabolite profiles were found in *crtI* lines

In order to assess the effect of crtI activity on the metabolome of tomato fruit, multi-platform metabolite profiling was carried out. Polar and non-polar metabolites were analysed using a number of targeted and non-targeted analytical platforms. The data shown in Table 3 were then subjected to Principal Component Analysis (PCA), (Figure S4). The PCA not only

discriminates the AC background from the *tangerine* background, but also *crtI* expression in either background from the relative wild type control. Through the comparisons of the AC background with AC:*crtI*, AC with t^{3183}, t^{3183} with *t*:*crtI* and AC with *t*:*crtI*, the main effects of crtI on the metabolome can be deciphered (Table 3) and visualised using pathway displays (Figure S5 A, B, C and D).

Changes in polyphenols were observed between genotypes. When present in the AC background, crtI resulted in elevated levels, due to increased chlorogenic acid, 5-caffeoylquinic acid and rutin. These changes were not evident when *crtI* was expressed in the t^{3183} background and compared to t^{3183} or AC controls. In this instance, the predominant flavonoid altered was naringenin-chalcone (5 and 3-fold increases relative to t^{3183} and AC, respectively).

Significant changes to phytosterols were observed, both in the presence of crtI, but also in the *tangerine* mutant relative to AC. For example, the ripe fruit from t^{3183} contained less phytosterols (campesterol, stigmasterol and cycloartenol) and the triterpenoid β-amyrin. The presence of crtI increased phytosterol content, predominantly cycloartenol (3-fold) and stigmasterol (2-fold), in t^{3183}. It also increased the levels of β-amyrin (2-fold) and phytosterols, predominantly cycloartenol, (2-fold) in the AC background.

Among the organic acids analysed, differences between the AC and t^{3183} were significant, with all TCA cycle intermediates increased apart from succinic acid. CrtI had the effect of reducing the TCA intermediates, in both backgrounds. Cell wall derived organic acids were also reduced in the t^{3183} mutant. In the AC background, crtI reduced levels, while in the t^{3183} background no significant reduction was observed. The content of ascorbic acid, and its derivatives, increased in the presence of crtI, but only in the AC background. With the

exception of cysteine in the AC background, which increased ~5-fold, the overriding feature of the amino acid content of fruit from either background was a significant reduction in levels. The predominant fatty acids palmitic, linoleic and steric acid showed a significant reduction when *crtI* was expressed in t^{3183}. In response to the presence of crtI, the sugars analysed displayed significant alterations in their levels. For example, rhamnose, sucrose and sedoheptulose all increased independently of the background. Glucose was consistently reduced, as was melizitose in both backgrounds. Also significantly reduced in both backgrounds by the effect of crtI were the polyols glycerol and inositol. These findings were typically replicated when in the phosphate form, for example inositol-6-phosphate.

Transgenic *old gold crimson* (*og*^{c}) tomato fruit expressing *crtI* contain elevated β–carotene levels

In order to investigate further the induction of β-carotene formation upon increased crtI activity, the *og*^{c} mutant, possessing a defective *CYCB*, was transformed with the *crtI* gene. Twenty-four primary transgenic lines expressing *crtI* were obtained. Analysis by Southern blotting identified 9 lines containing single inserts, the rest containing multiple inserts. Those containing *crtI* were designated *og*^{c}:*crtI*-1 to 24 and compared to their control *og*^{c} allele in the Ailsa Craig (AC) background.

The predominant carotenoids present in ripe fruit from 24 primary *og*^{c}:*crtI* lines were quantified (Table S6). The profiles were variable between individual transformation events, but those lines containing increased β-carotene levels (2 to 6-fold), all displayed significant reductions (55-80%) in both phytoene and phytofluene, similar to that observed in the t^{3183} and AC backgrounds expressing *crtI*. Two single insert lines (og^c:*crtI*-20 and 22; Table S6) were identified as maintaining high lycopene levels, in addition to having significantly

elevated β-carotene content (4.6 and 6-fold increases relative to og^c). These lines were used to generate a T1 population.

Ripe fruit from the T1 generation were profiled for carotenoid content compared to the og^c background (Table S7). The homozygous lines maintained og^c levels of lycopene, whilst accumulating up to 2-fold the og^c level of β-carotene (Table 1C and Table S7). Only two homozygous lines were identified as having no change/a decrease in β-carotene content. Hemizygous lines, however, were more inconsistent in their lycopene and β-carotene content and although some contained the highest levels of β-carotene (up to 4-fold og^c level), there was no consistent trend observed, with some lines showing increases and others decreases, or wild type levels in either β-carotene or lycopene. There was also no clear correlation, in the hemizygous lines, between β-carotene content and lycopene levels.

Comparison of the og^c gene expression profile with the wild type showed a down regulation of early pathway genes including *DXS*, *GGPPS*2, *PSY*1 and *PSY*2, *ZDS* and *CRTISO,* but an increase in the expression of the epsilon-cyclase, *LCYE*, and the chloroplast specific β-cyclase, *LCYB* (Figure 3). Expression of *crtI* in the og^c background resulted in the further induction of *LCYB*, as seen in AC:*crtI*, as well as a further reduction in the expression of both phytoene synthase genes, as shown in AC:*crtI*. In both the AC and t^{3183} backgrounds, expression of *crtI* resulted in significant increases in the expression of *LCYE*. No such increase was seen in the og^c:*crtI* lines; however the expression level of *LCYE* in og^c was already significantly higher than in AC.

DISCUSSION

crtI in the *tangerine* mutant overcomes impaired desaturation/isomerisation

The *tangerine* mutant used in this study, t^{3183}, does not express the *CRTISO* gene and as a result the desaturation/isomerisation of phytoene is impaired (Isaacson et al., 2002, 2004). Functional expression of *crtI* in the *t*:*crtI* transformants has overcome the impaired desaturation/isomerisation (Table 1, Table S1 and Figure S2). Prolycopene is the end product of phytoene desaturation in plants and algae (Zechmeister et al., 1941; Breitenbach and Sandmann, 2005); (Figure 1). In *CRTISO* mutants of *Arabidopsis* and tomato, prolycopene has been reported to accumulate (Isaacson et al., 2002; Park et al., 2002). In the present study, the *tangerine* mutant accumulated phytoene, predominantly the 15-*cis* geometric isomer (98%), ζ-carotene, neurosporene and then prolycopene, but not β-carotene; this steady state profile was corroborated *in vitro*. The *CRTISO* transcript was at ~0.008-fold the level of AC (Figure 2). This profile corresponds to that observed from transient VIGS studies with *CRTISO* in fruit (Fantini et al., 2013). Thus, it would appear that CRTISO is not solely restricted to the isomerisation of prolycopene, but also isomerises other intermediates such as ζ-carotene in the desaturation series.. Alternatively, phytoene and ζ-carotene desaturation are subject to feedback inhibition and will not proceed if *cis* isomers accumulate. When present in the AC background, crtI altered the pigment profile by reducing the presence of *cis* isomers in the desaturation sequence to virtually zero (Table 1C) and instead of lycopene, β-carotene predominated. These data are supported by *in vitro* assays that demonstrated increased desaturase and cyclase activity and similar *in vitro* product profiles (Table 2 andS5). A similar situation was observed when *crtI* was expressed in the *tangerine* mutant (Table 1C, Table S1 and Figure S2). Firstly, the levels of *cis* carotene isomers were reduced, but not eliminated. Although all-*trans* lycopene was detected, β-carotene predominated, thus

enforcing a previous study reporting prolycopene cannot be cyclised (Yu et al., 2011). The *in vitro* data supported the profiles found with the steady state metabolites, with the exception that the increases in cyclase-specific enzyme activity was not observed, but was evident when phytoene was used as the precursor. Another explanation could be that the crtI competes with the plant desaturation and *cis* isomers are reduced because the plant based desaturation has to perform in a more effective manner. However, this is unlikely as in the t^{3183} where the mutation prevents isomerisation, *cis* isomers are reduced in the presence of the crtI. Thus, on the basis of the experimental data acquired, the crtI desaturase/isomerase can: (i), access its precursor 15-*cis* phytoene *in vivo* and *in vitro*; (ii), perform *cis*-*trans* isomerisation throughout the desaturation sequence within the plastid microenvironment; (iii), interact and co-exist with the endogenous plant desaturase and (iv), produce all-*trans*-lycopene that is the exclusive substrate *in vivo* for cyclisation to β-carotene via γ-carotene. The evolution of the carotene desaturases and the relationship to isomerase function within the pathway has been postulated (Sandmann, 2009)

The presence of crtI, in both the AC and *tangerine* backgrounds, resulted in β-carotene formation (Table 1C). This was corroborated by the *in vitro* products from phytoene (Table S5), but the specific cyclase activity in the *t*:*crtI* did not significantly increase compared to the parent (Table 2), suggesting the substrate was not accessible. This may have important connotations for enzyme topology. For example, Shumskaya and Wurtzel (2013) and Nogueira et al. (2013) have provided models for the interaction and location of the enzymes. The latter demonstrated that phytoene was accessible to the crtI protein, but in excess was compartmentalised into plastoglobules and the crtI and cyclase have a closer topological interaction than that of the native desaturation complex and cyclase.

Comparison between the *t*:*crtI* data and AC:*crtI* data corroborate these conclusions and a disturbed plant desaturation/isomerisation complex may aid the crtI-/cyclase interaction.

Why and how do changes in carotene levels alter pathway transcription and enzyme activities?

The end product of the crtI catalysed reaction is all-*trans*-lycopene (with some didehydrolycopene). However, β-carotene accumulation increases in tomato lines expressing *crtI* (Romer et al., 2000; Table 1C). This is due to the induction of lycopene β-cyclase transcripts and increased enzyme activity converting all-*trans* lycopene into β-carotene (Figure 2, Table S4, Figure S3 and Table2). It is interesting to note that in the case of the t^{3183}, the presence of crtI results in the induction of the ripening-specific lycopene cyclase. However, in the og^{c} mutant, which has a null fruit β-lycopene cyclase, the constitutive β-lycopene cyclase is induced. Figure 4 summarises and emphasises the differential expression that arises between the cyclases in response to the crtI in different genotypes. Therefore, crtI increases the pool of lycopene, which creates a feed forward loop, resulting in the transcriptional activation of cyclase genes. These changes are then translated, as the enzyme activity is increased. In addition to the β-cyclases, the expression of the ε-cyclase is also increased, and lutein content in the fruit elevated. In the vegetative tissues of tomato the up-regulation of the *CYCB* was observed in the presence of *crtI* expression (Nogueira et al., 2013). Previous reports in vegetative tobacco tissue also indicate that the *crt*I could alter β-ring derived xanthophylls presumably via the induction of lycopene β-cyclases (Misawa et al 1994). This change in β-ring derived xanthophylls, at the expense of lutein could also have had effect on chlorophyll content due to their association in the photosynthetic complexes. Such effects appeared to be more pronounced in mature green fruit, where unlike the leaf tissue chlorophyll content was reduced to levels where the ratio of chlorophyll:carotenoids

was effected. In contrast to transcriptional induction, the majority of the pre-phytoene desaturase enzymes and their transcripts show reduced activity and a poor correlation between transcript and enzyme activity levels (Table2, Figure 2). This could indicate a significant role for post-transcriptional regulation of the pathway. Recently, the interaction of the *Arabidopsis* phytoene synthase with the OR protein has been demonstrated and proposed as a key regulatory mechanism controlling the synthesis of phytoene (Zhou et al., 2015). Such perturbations display consistent trends across the AC, t^{3183} and og^{c} backgrounds. Thus, when a precursor in the pathway is increased or decreased within the plastid organelle, it transmits a signal to facilitate increased transcription in the nucleus, leading to increased protein/enzyme activity in most cases. These processes and mechanisms await elucidation, but recently several retrograde signals from the plastid have been postulated. These include *cis*-carotene via the action of CCDs as speculated in (Kachanovsky et al., 2012) and proposed in Avendano-Vazquez et al., 2014. In addition carotenoid oxygenation products such as β-cyclocitral (Ramel et al., 2012) and MEP intermediates (Walley et al., 2015) have been proposed. In the present study, crtI has been shown to metabolise acyclic *cis*-carotenes involved in desaturation, reducing levels and presumably restricting the action of CCDs in the generation of apocarotenoid signalling molecules. No phenotype changes are observed, suggesting these apocarotenoids are not involved in retrograde signalling responsible for pathway regulation in fruit. However, the increases in β-carotene could plausibly generate β-cyclocitral, which has the potential to act a pathway modulator . MEP intermediates are more polar and therefore more likely to exit the plastid organelle. However, it is more probable, from their chemical nature and biosynthetic location of the enzymes that the MEP pathway would interact with perturbations in intermediary metabolism and drive isoprenoid formation in this manner. The increased tocopherol level arising from the presence of crtI activity (Figure S3) is likely to be linked to GGPP utilisation. In this case, crtI results in reduced

phytoene, but increased expression of *GGPPS1*, indicates the diversion of GGPP into the tocopherol pathway. Such biochemical interaction between the carotenoid and tocopherol pathways suggests the pathways and their intermediates are in close spatial proximity.

Nogueira et al. (2013) reported changes in plastidial membrane lipids, resulting from perturbations in carotenoid levels and composition. Thus, it is feasible that lipid-derived compounds could also contribute to the sensing of pathway modulation by the nuclear location transcriptional regulation (Kobayashi et al., 2014). Finally, proteomic studies have revealed a number of membrane localised transcription factors and proteases (Adam, 2013; Lyska et al., 2013). These components could operate in a mechanism akin to that elucidated for cholesterol biosynthesis (Brown and Goldstein, 1997), whereby protein/lipid interactions sense the level of carotenoids embedded in the membrane and trigger the transmission of the signal to the nucleus.

Changes to the metabolome resulting from the modulation of phytoene desaturation

Although the primary target for the manipulations performed in this study were associated with the carotenoid pathway, metabolite levels across intermediary metabolism were analysed (Table 3). Previous studies have illustrated that intermediary metabolism can be the progenitor for secondary metabolites (Enfissi et al., 2010). Large-scale global metabolomic studies and correlations across introgression populations have revealed the interconnectivity of primary, intermediary and secondary metabolism (Perez-Fons et al., 2014). Finally, perturbations in tomato fruit carotenoid formation have been shown to affect steady state levels of intermediary metabolites (Enfissi et al., 2010). The latter is likely to be the case in the present study and these data illustrate that it is naïve to view sectors of metabolism as isolated entities. Instead, they are components of a larger network. Potentially,

the altered levels of intermediary metabolites associated with the changes in carotenes could facilitate the supply of precursors or reductant, as enhanced flux into the pathway is required. It is also possible that some of the metabolites and/or carotenoids themselves are bioactive components that alter physiological/developmental processes and as a consequence the levels of associated metabolites are altered. For example, the changes in carotenoids may alter phytohormones such as abscisic acid (ABA), cytokines, or gibberellins. The carotenoids may also alter the efficiency of photosynthesis, leading to altered sugar levels and instigate sensing pathways. Associated with this hypothesis, is the recent study showing how a transcription factor, responsible for the dramatic increases in flavonols and hydroxycinnamates in ripe tomato fruit, can also directly up-regulate transcripts/enzymes involved in primary metabolism that supplies precursors, energy and reducing power for secondary metabolism (Zhang et al. 2015). In the present study it would appear that a similar effect is occurring but initiated solely by increased biosynthetic capacity in the carotenoid pathway, suggesting a role for the modulation by metabolites across intermediary metabolism. Further Systems Biology approaches will hopefully provide future insights into the modulation of metabolism by small molecules derived from the perturbation of the carotene pathway.

In conclusion, the studies presented provide valuable insights into the sequence of carotene desaturation/isomerisation in plants and how crtI can interact with the process *in vivo*. In addition, the ability and complexity of the pathway to regulate carotenoid content via feedback and feed-forward mechanisms have been revealed. Despite the manipulation being targeted to the carotenoid pathway, global effects on the metabolome arose, illustrating the interconnectivity of metabolism. Given the importance of crtI in "Golden Rice" and its utility to engineering carotene desaturation with one gene instead of four, these studies have

provided ~~new~~ fundamental data with biotechnological applications. Further detailed studies are now required to reveal the signalling/sensing mechanisms associated with the ability of plant tissues to regulate the pathway at multiple cellular levels. The germplasm generated will provide a valuable resource to address these hypotheses.

EXPERIMENTAL PROCEDURES

Plant material and the generation of transgenic tomato plants expressing a bacterial *crtI*

The *tangerine* (t^{3183}) and *old gold crimson* (og^{c}) mutants of tomato (accessions LA3183 and LA3179, respectively) were transformed with the construct described by (Romer et al., 2000), containing the *crtI* from *Pantoea ananatis* under the control of the 35S promoter and *NPTII* for kanamycin selection. A standard *Agrobacterium*-mediated transformation method, as described previously (Bird et al., 1988), was used. Kanamycin selection and PCR screening (as described below) for the presence of the transgene were used to identify positive transformants. All plants were grown under identical conditions in a glasshouse, as described in Romer et al. (2000).

Genotyping

Genomic DNA was extracted from leaf material using Qiagen DNeasy plant mini kit (Qiagen Ltd. Crawley UK) using the manufacturer's standard protocol. Genomic DNA (25 ng) was then used as template for PCR using primers specific to *P. ananatis crtI* (primer sequences provided in Supporting Information - Table S8). For Southern blotting, genomic DNA (10 μg) was digested using EcoRI or HindIII and fragments separated on a 0.8% (w/v) agarose gel and then blotted onto positively charged nylon membrane. Blots were probed with a PCR derived *NPTII* fragment incorporating a digoxigenin-11-dUTP label (Roche

Diagnostics Ltd., Burgess Hill UK). Primers used to amplify the probe sequence are provided in Supporting Information - Table S8.

Gene expression analysis

Total RNA was extracted for use in quantitative real time reverse transcriptase PCR (qRT-PCR) using Qiagen RNeasy plant mini kit (Qiagen Ltd. Crawley UK) using the manufacturer's protocol, including on-column DNaseI digestion. The QuantiTect SYBR Green, one-step real-time RT-PCR kit (Qiagen, Ltd., Crawley, UK) was used to determine gene expression levels. Determinations used RNA (25 ng) extracted from pooled samples taken from a minimum of 3 biological replicates. Reactions were performed on a Rotor-Gene 3000 thermocycler (Qiagen, Ltd., Crawley, UK). Thermocycling conditions were 30 min 50^{o}C for reverse transcription, 15 min at 95^{o}C, followed by 30 to 40 cycles of 15 s at 94 ^{o}C, 30 s at 56 ^{o}C, and 30 s, 76 ^{o}C. Sequencing of PCR products, as well as melt curve analyses, verified reaction specificity. For quantification, calibration curves were run simultaneously with experimental samples, and Ct calculations were performed by the Rotor-Gene software. The actin gene served as reference for normalisation. Primers for quantitative real-time RT-PCR were designed using Primer3 software (http://primer3.sourceforge.net/) and are provided in Supporting Information - Table S8.

Immunodetection

Proteins for immunodetection were separated by SDS-PAGE and electroblotted onto polyvinylidene difluoride (PVDF) membranes. Immunodetection was carried out as described in (Fraser et al., 1994), using polyclonal crtI antibodies (Fraser et al., 1992).

Preparation of cell-free and plastid extracts

Phycomyces blakesleeanus extracts of mutants capable of producing phytoene (*carB*) and lycopene (*carR*) *in vitro* were prepared from freeze-dried mycelia, as described previously (Bramley, 1973). The preparation of crude plastid fractions from ripe fruit for the assay of carotenogenic enzymes was performed using the procedures described in Fraser et al. (1994). In the present study, crude chromoplast preparations from ripening tomato fruit (3 to 4 days post-breaker) were fractionated by centrifugation following breakage by osmotic shock in 0.4 M Tris-HCl pH 8.0 buffer, containing 1 mM DTT. The resulting suspension was centrifuged at 105 000*g* to generate a supernatant designated the stromal preparation and particular membrane fraction. Based on validation experiments (Fraser et al., 1994; 2002), stromal extracts (200 mL) were used for the determination of phytoene synthase activity and the re-suspended membrane fraction (0.4 M Tris-HCl pH 8.0 buffer, containing 1 mM DTT) used for phytoene metabolising activities.

Enzyme assays

The determinations of carotenoid enzyme activities using established techniques have been detailed previously in Fraser et al. (2007). In brief, DXS activity was measured using 0.25 mCi [2-^{14}C] pyruvate (30 mci/mmol: ICN) as the substrate. The incubation mixture (200 μL) was buffered with 0.4 M Tris-HCL pH 8.0 containing 1 mM DTT, 3 mM ATP, 2 mM $MgSO_4$, 2 mM $MnCl_2$, 1 mM KF, 0.1%w/v Tween 60, 1 mM thiamine and 4 mM *D*-glyceraldehyde-3-phosphate. Initiation of the reaction was carried out with the addition of the plastid/stroma fraction (200 μL). Isopentenyl pyrophosphate isomerase (IPI) activity was determined using 0.25 mCi [1-^{14}C-IPP], (56 mCi/mmol, Amersham) as the substrate. A similar incubation solution to that used for DXS was implemented, except thiamine and *D*-glyceraldehyde-3-phosphate was omitted. In order to terminate the incubation, methanol (200

μL) was added and acid hydrolysis performed by adding HCl to a final concentration of 25% then incubated for 1 h at 37^{o}C with shaking at 100 rpm. In the case of GGPP synthase identical conditions to those used for IPI were used except dimethylallyl diphosphate (DMAPP) in addition to radiolabelled IPP was added. DMAPP was added from a 200 mM stock (prepared in methanol) until a final concentration of 2 mM was reached. Phytoene synthase activity was directly assayed using the plastid stroma fraction prepared in 0.4 M Tris-HCl pH 8.0 as the source. The substrate used was 0.5 mCi [^{3}H]-GGPP, (15 mCi/mmol, American Radiolabeled Chemicals), the incubation mixture was similar to GGPP synthase and is detailed in Fraser et al. (2000a). In the case of phytoene desaturation and lycopene cyclisation, a coupled assay system was used as described previously (Fraser et al., 1991; 1994 and 2002).

DXS reaction products and precursors were separated on normal phase TLC plate (Silica gel 60; VWR). The mobile phase used was isopropanol:ethyl acetate:water (6:1:3). Deoxyxylulose (DX) and deoxyxylulose phosphate (DXP) where identified by co-chromatography. Radioactive compounds were localised by autoradiography (x-ray hyperfilm, VWR). Quantitation was achieved by scraping the zones from the thin layer and the amount of radioactivity determined by liquid scintillation counting.

The reaction products from IPI and GGPP synthase assays, as well as the incorporation of ^{14}C-IPP, were analysed as described in Fraser et al. (2007). Incorporation into phytoene was determined by separation on activated aluminium oxide TLC plates developed in 6% v/v toluene in petroleum ether 40-60^{o}C for approximately 1 h. After air drying, the plate was stained in iodine to localise the position of phytoene. The radioactivity present was determined by scraping the stationary phase from the plate and into scintillation

fluid (3 mL) ready for scintillation counting. The prenyl phosphates present in the aqueous phase were converted to their alcohol derivatives by acid hydrolysis as described above. . Individual components were separated by TLC using a silica based reversed-phase (C_{18}) stationary phase that was developed in a methanol:water (95:5) mobile phase. Prior to separation, the appropriate authentic standards were added to the extracts and the solvent dried under nitrogen gas. Following development, the localisation of dimethylallyl alcohol, geraniol, farnesol, geranylgeraniol and phytol was determined by staining in iodine. R_F values for these compounds on this system were 0.82, 0.61, 0.45, 0.32 and 0.19, respectively. The stained zones/prenyl alcohols were scraped off the thin layers mixed with scintillation fluid (3 mL) and the amount of radioactivity incorporated determined by liquid scintillation counting. The phytoene produced from the specific phytoene synthase assay was determined as described for the organic extracts derived from the ^{14}C-IPP incorporation. Following extraction with methanol:chloroform (1:2 v/v) and subsequent re-extraction, the radiolabelled desaturase products present were separated and quantified by TLC and scintillation counting, respectively (Fraser et al.,1994 and 2002).

Metabolite analyses

The extraction of carotenoids and tocopherols was performed on lyophilised tissue that had been milled to a fine powder. Ground, homogeneous tissue (10 mg) was extracted with chloroform and methanol (2.5:1 v/v), (Fraser et al. 2000b). Separation and detection by HPLC-PDA of individual components was performed using two systems. Both used a C_{30} reverse-phase column (250 x 4.6 mm; YMC, Wilmington, NC). HPLC-I system has been described in detail previously (Fraser et al., 2000b). System HPLC-II was developed to achieve baseline separation of β-carotene and prolycopene. In system HPLC-II, the column temperature was 10^{o}C. The mobile phases were methanol (A), water (B), and *tert*-methyl

butyl ether (C). The gradient used was 95% A : 5%B, isocratically for 6 min and then stepped to 60%A : 5%B : 35%C for 5 min , from which a linear gradient to 15%A : 5%B : 80%C over 20 min was performed and held for 16 min, after which it returned to 95%A : 5%B over 2 min and held for 10 min. A Waters Alliance model 2695 (Waters Ltd., Watford Herts.) injection and solvent delivery system was used. Detection was performed continuously from 220-700 nm with an online PDA (Waters 966, Waters Limited, Watford, Herts). Identification was carried out by co-chromatography and comparison of spectral properties with authentic standards and reference spectra (Fraser et al., 2000b). Quantitative determination of carotenoids was performed by comparison with dose-response curves (0.2 to 1.0 μg) constructed from authentic standards.

Procedures used to extract, separate, detect and quantify phenylpropanoids and flavonoids from lyophilised tomato material were followed as described by Davuluri et al. (2005) and Long et al. (2006). Total phytosterols were routinely extracted from finely milled tomato powder (20 mg), as described in Enfissi et al. (2010) using β-cholestanol as an internal standard.

Metabolites for GC-MS analysis were routinely extracted from finely milled tomato powder (20 mg) and derivatised as described in Enfissi et al. (2010) using ribitol (20 mg/mL) as an internal standard. GC-MS analysis was carried out on an Agilent HP6890 GC with a 5973MSD. Typically samples (1μL) were injected with a split/splitless injector at 290^{o}C with a 20:1 split and repeated on a 200:1 split for sugar quantification. Retention time locking (RTL) to the internal standard was used. The GC oven was held for 4 min at 70^{o}C before ramping at 5^{o}C/min to 310^{o}C. This final temperature was held for a further 10 min. The interface with the MS was set at 290^{o}C and MS performed in full scan mode using 70eV EI+

and scanned from 10-800 Da. In order to identify chromatogram components found in the tomato profiles, mass spectral (MS) library was constructed from in-house standards as well as the NIST 98 mass spectral library. Chromatogram components were initially processed by Automated Mass Spectral Deconvolution and Identification System (AMDIS). A retention time calibration was performed on all standards to facilitate the determination of retention indices (RIs). Using the RIs an MS identification was performed by comparison with the MS library. Quantification was achieved using ChemStation (Agilent) software facilitating integrated peak areas for specific compound targets (qualifier ions) relative to the ribitol internal standard peak.

Data Processing and statistical treatment

All experiments typically used a minimum of three biological and three technical replicates unless stated otherwise. PCA analysis was performed on these data matrixes. SPSS software (version 12.01) and SIMCA-P+ (Umetrics) were used to carry out and display clusters derived from PCA analyses. One-way ANOVA or Student's *t* tests were used as appropriate to determine significant differences between pairwise comparisons among the transgenic lines and their controls and between the natural mutants (t^{3183} and og^{c}) and the wild type (AC) background. Where appropriate, $P < 0.05$, $P < 0.01$, and $P < 0.001$ are indicated by *, **, and ***, respectively. One-way ANOVA, Student's *t* tests, means, and standard deviations were all calculated using GraphPad Prism software (GraphPad Software) or Excel (Microsoft) embedded algorithms. The overlaying of metabolite data over biochemical pathways was performed using BioSynLab software (www.biosynlab.com) from csv Excel files.

ACCESSION NUMBERS

Sequence data from this article can be found in the GenBank/EMBL databases under the accession numbers presented in Supporting Information - Table S8.

ACKNOWLEDGEMENTS

This work was supported in part through the European Union Framework Program FP5 ProVitaminA, FP7 Metapro No 244348 and DISCO projects No 613513. We thank Mr Chris Gerrish for technical assistance with immunodetection experiments.

AUTHOR CONTRIBUTIONS

EMAE and PDF performed the experiments. PDF, EMAE and PMB designed the research program. PDF and EMAE wrote the article. MN contributed materials to the work and interpretation of the data. PMB and PDF acquired the funding.

CONFLICT OF INTEREST

The authors declare that they have no competing commercial interests in relation to this work.

SUPPORTING INFORMATION LEGENDS

Figure S1. Phenotypical ripe fruit from (A) *tangerine* plants and (B) *tangerine* plants expressing *crtI***.**

Figure S2. Typical HPLC chromatograms of ripe *t:crtI* fruit recorded at 450 nm using two HPLC-PDA systems.

Figure S3. (A) Expression of genes involved in tocopherol biosynthesis, (B) tocopherol levels and (C) incorporation of ^{14}C-IPP into prenyl lipids, phytol and phytoene in 3 days post

breaker fruit from Ailsa Craig control (AC), AC expressing *crtI* (AC:*crtI*), *tangerine* control (t^{3183}) and a stable homozygous t^{3183} line expressing *crtI* (*t*:*crtI*-9-11).

Figure S4. Principle Component Analysis of polar extracts from ripe fruit of the wild type (AC), Tangerine (t^{3183}), AC:*crtI*, and *t*:*crtI* varieties.

Figure S5. (A) Changes in metabolites occurring in ripe fruit of Ailsa Craig plants expressing *crtI* relative to Ailsa Craig (B) Changes in metabolites occurring in ripe fruit of *tangerine*, t^{3183}, plants as a result of a defective *CRTISO* gene relative to AC. (C) Changes in metabolites occurring in ripe fruit of *tangerine* plants expressing *crtI* relative to the tangerine background. (D) Changes in metabolites occurring in ripe fruit of *tangerine* plants expressing *crtI* relative to the Ailsa Craig background.

Table S1. Retention times and spectral characteristics (in the eluting solvent) used in identification of isoprenoids separated by HPLC-PDA and two TLC systems.

Table S2. The levels of the predominant carotenoids in ripe pericarp tissue from primary t^{3183} plants transformed with the *crtI* gene.

Table S3. The levels of predominant pigments in ripe pericarp tissue from wild type (AC), AC expressing *crtI* (AC:*crtI*) and the T1 generation of plants grown from four independent, single-insert primary t^{3183} plants expressing *crtI*.

Table S4. Carotenoid pathway gene expression levels in 3 day post breaker fruit from lines expressing *crtI* relative to their specific backgrounds.

Table S5. The proportion of individual desaturase products formed *in vitro* from phytoene in varieties with altered carotene desaturation and isomerisation.

Table S6. The levels of the predominant carotenoids in ripe pericarp tissue from primary og^{c} plants transformed with *crtI*.

Table S7. The levels of predominant pigments in ripe pericarp tissue from the T1 generation of plants grown from two independent, single-insert, primary *og*^{c} plants expressing *crtI*.

Table S8. Sequences of primers used in real-time RT-PCR and PCR.

REFERENCES

Adam, Z. (2013). Emerging roles for diverse intramembrane proteases in plant biology. Bba-Biomembranes **1828,** 2933-2936.

Avendano-Vazquez, A.O., Cordoba, E., Llamas, E., San Roman, C., Nisar, N., De la Torre, S., Ramos-Vega, M., Gutierrez-Nava, M.D., Cazzonelli, C.I., Pogson, B.J., and Leon, P. (2014). An Uncharacterized Apocarotenoid-Derived Signal Generated in zeta-Carotene Desaturase Mutants Regulates Leaf Development and the Expression of Chloroplast and Nuclear Genes in *Arabidopsis*. Plant Cell **26,** 2524-2537.

Beltran, J., Kloss, B., Hosler, J.P., Geng, J., Liu, A., Modi, A., Dawson, J.H., Sono, M., Shumskaya, M., Ampomah-Dwamena, C., Love, J.D., and Wurtzel, E.T. (2015). Control of carotenoid biosynthesis through a heme-based cis-trans isomerase. Nat Chem Biol **11,** 598-605.

Bird, C.R., Smith, C.J., Ray, J.A., Moureau, P., Bevan, M.W., Bird, A.S., Hughes, S., Morris, P.C., Grierson, D., and Schuch, W. (1988). The tomato polygalacturonase gene and ripening-specific expression in transgenic plants. Plant Mol Biol **11,** 651-662.

Breitenbach, J., and Sandmann, G. (2005). zeta-Carotene cis isomers as products and substrates in the plant poly-cis carotenoid biosynthetic pathway to lycopene. Planta **220,** 785-793.

Brown, M.S., and Goldstein, J.L. (1997). The SREBP pathway: Regulation of cholesterol metabolism by proteolysis of a membrane-bound transcription factor. Cell **89,** 331-340.

Chen, Y., Li, F., and Wurtzel, E.T. (2010). Isolation and characterization of the Z-ISO gene encoding a missing component of carotenoid biosynthesis in plants. Plant Physiol **153,** 66-79.

Davuluri, G.R., van Tuinen, A., Fraser, P.D., Manfredonia, A., Newman, R., Burgess, D., Brummell, D.A., King, S.R., Palys, J., Uhlig, J., Bramley, P.M., Pennings, H.M., and Bowler, C. (2005). Fruit-specific RNAi-mediated suppression of DET1 enhances carotenoid and flavonoid content in tomatoes. Nat Biotechnol **23,** 890-895.

Demmig-Adams, B., and Adams, W.W., 3rd. (2002). Antioxidants in photosynthesis and human nutrition. Science **298,** 2149-2153.

Enfissi, E.M., Barneche, F., Ahmed, I., Lichtle, C., Gerrish, C., McQuinn, R.P., Giovannoni, J.J., Lopez-Juez, E., Bowler, C., Bramley, P.M., and Fraser, P.D. (2010). Integrative transcript and metabolite analysis of nutritionally enhanced DE-ETIOLATED1 downregulated tomato fruit. Plant Cell **22,** 1190-1215.

Fantini, E., Falcone, G., Frusciante, S., Giliberto, L., and Giuliano, G. (2013). Dissection of tomato lycopene biosynthesis through virus-induced gene silencing. Plant Physiol **163,** 986-998.

Fraser, P.D., and Bramley, P.M. (2004). The biosynthesis and nutritional uses of carotenoids. Prog Lipid Res **43,** 228-265.

Fraser, P.D., Linden, H., and Sandmann, G. (1993). Purification and reactivation of recombinant *Synechococcus* phytoene desaturase from an overexpressing strain of Escherichia coli. Biochem J **291 (Pt 3),** 687-692.

Fraser, P.D., Schuch, W., and Bramley, P.M. (2000a). Phytoene synthase from tomato (*Lycopersicon esculentum*) chloroplasts--partial purification and biochemical properties. Planta **211,** 361-369.

Fraser, P.D., Pinto, M.E., Holloway, D.E., and Bramley, P.M. (2000b). Technical advance: application of high-performance liquid chromatography with photodiode array detection to the metabolic profiling of plant isoprenoids. Plant J **24,** 551-558.

Fraser, P.D., Truesdale, M.R., Bird, C.R., Schuch, W., and Bramley, P.M. (1994). Carotenoid Biosynthesis during Tomato Fruit Development (Evidence for Tissue-Specific Gene Expression). Plant Physiol **105,** 405-413.

Fraser, P.D., Misawa, N., Linden, H., Yamano, S., Kobayashi, K., and Sandmann, G. (1992). Expression in *Escherichia coli*, purification, and reactivation of the recombinant *Erwinia uredovora* phytoene desaturase. J Biol Chem **267,** 19891-19895.

Fraser, P.D., Enfissi, E.M., Halket, J.M., Truesdale, M.R., Yu, D., Gerrish, C., and Bramley, P.M. (2007). Manipulation of phytoene levels in tomato fruit: effects on isoprenoids, plastids, and intermediary metabolism. Plant Cell **19,** 3194-3211.

Gemmecker, S., Schaub, P., Koschmieder, J., Brausemann, A., Drepper, F., Rodriguez-Franco, M., Ghisla, S., Warscheid, B., Einsle, O., and Beyer, P. (2015). Phytoene Desaturase from *Oryza sativa*: Oligomeric Assembly, Membrane Association and Preliminary 3D-Analysis. PloS one **10,** e0131717.

Hirschberg, J. (2001). Carotenoid biosynthesis in flowering plants. Curr Opin Plant Biol **4,** 210-218.

Isaacson, T., Ronen, G., Zamir, D., and Hirschberg, J. (2002). Cloning of tangerine from tomato reveals a carotenoid isomerase essential for the production of beta-carotene and xanthophylls in plants. Plant Cell **14,** 333-342.

Isaacson, T., Ohad, I., Beyer, P., and Hirschberg, J. (2004). Analysis in vitro of the enzyme CRTISO establishes a poly-*cis*-carotenoid biosynthesis pathway in plants. Plant Physiol **136,** 4246-4255.

Kachanovsky, D.E., Filler, S., Isaacson, T., and Hirschberg, J. (2012). Epistasis in tomato color mutations involves regulation of phytoene synthase 1 expression by cis-carotenoids. Proc Natl Acad Sci U S A **109,** 19021-19026.

Kobayashi, K., Fujii, S., Sasaki, D., Baba, S., Ohta, H., Masuda, T., and Wada, H. (2014). Transcriptional regulation of thylakoid galactolipid biosynthesis coordinated with chlorophyll biosynthesis during the development of chloroplasts in *Arabidopsis*. Front Plant Sci **5**.

Krinsky, N.I., and Johnson, E.J. (2005). Carotenoid actions and their relation to health and disease. Mol Aspects Med **26,** 459-516.

Linden, H., Misawa, N., Chamovitz, D., Pecker, I., Hirschberg, J., and Sandmann, G. (1991). Functional complementation in *Escherichia-coli* of different phytoene desaturase genes and analysis of accumulated carotenes. Z.Naturforsch.(C) **46,** 1045-1051.

Long, M., Millar, D.J., Kimura, Y., Donovan, G., Rees, J., Fraser, P.D., Bramley, P.M., and Bolwell, G.P. (2006). Metabolite profiling of carotenoid and phenolic pathways in mutant and transgenic lines of tomato: identification of a high antioxidant fruit line. Phytochemistry **67,** 1750-1757.

Lyska, D., Meierhoff, K., and Westhoff, P. (2013). How to build functional thylakoid membranes: from plastid transcription to protein complex assembly. Planta **237,** 413-428.

Misawa, N., Masamata, K., Hori, T., Ohtani, T., Boeger, P., and Sandmann G. (1994). Expression of an *Erwinia* phytoene desaturase gene not only confers multiple

resistance to herbicides interfering with carotenoid biosynthesis but also alters xanthophyll metabolism in transgenic plants. Plant J **6**, 481-489.

Nogueira, M., Mora, L., Enfissi, E.M., Bramley, P.M., and Fraser, P.D. (2013). Subchromoplast sequestration of carotenoids affects regulatory mechanisms in tomato lines expressing different carotenoid gene combinations. Plant Cell **25,** 4560-4579.

Park, H., Kreunen, S.S., Cuttriss, A.J., DellaPenna, D., and Pogson, B.J. (2002). Identification of the carotenoid isomerase provides insight into carotenoid biosynthesis, prolamellar body formation, and photomorphogenesis. Plant Cell **14,** 321-332.

Perez-Fons, L., Wells, T., Corol, D.I., Ward, J.L., Gerrish, C., Beale, M.H., Seymour, G.B., Bramley, P.M., and Fraser, P.D. (2014). A genome-wide metabolomic resource for tomato fruit from *Solanum pennellii.* Sci Rep **4,** 3859.

Pulido, P., Toledo-Ortiz, G., Phillips, M.A., Wright, L.P., and Rodriguez-Concepcion, M. (2013). *Arabidopsis* J-protein J20 delivers the first enzyme of the plastidial isoprenoid pathway to protein quality control. Plant Cell **25,** 4183-4194.

Ramel, F., Birtic, S., Ginies, C., Soubigou-Taconnat, L., Triantaphylides, C., and Havaux, M. (2012). Carotenoid oxidation products are stress signals that mediate gene responses to singlet oxygen in plants. Proc Natl Acad Sci U S A **109,** 5535-5540.

Rao, A.V., Fleshner, N., and Agarwal, S. (1999). Serum and tissue lycopene and biomarkers of oxidation in prostate cancer patients: a case-control study. Nutr Cancer **33,** 159-164.

Romer, S., Fraser, P.D., Kiano, J.W., Shipton, C.A., Misawa, N., Schuch, W., and Bramley, P.M. (2000). Elevation of the provitamin A content of transgenic tomato plants. Nat Biotechnol **18,** 666-669.

Ronen, G., Carmel-Goren, L., Zamir, D., and Hirschberg, J. (2000). An alternative pathway to beta-carotene formation in plant chromoplasts discovered by map-based cloning of Beta and old-gold color mutations in tomato. P Natl Acad Sci USA **97,** 11102-11107.

Sandmann, G., Ward, C.E., Lo, W.C., Nagy, J.O., and Boger, P. (1990). Bleaching herbicide flurtamone interferes with phytoene desaturase. Plant Physiol **94,** 476-478.

Sandmann G. (2009). Evolution of carotene desaturation: the complication of a simple pathway. Arch. Biochem. Biophys.;483,:169-74.

Schaub, P., Yu, Q., Gemmecker, S., Poussin-Courmontagne, P., Mailliot, J., McEwen, A.G., Ghisla, S., Al-Babili, S., Cavarelli, J., and Beyer, P. (2012). On the structure and function of the phytoene desaturase CRTI from *Pantoea ananatis*, a membrane-peripheral and FAD-dependent oxidase/isomerase. PLoS One **7,** e39550.

Schwartz, S.H., Qin, X., and Zeevaart, J.A. (2003). Elucidation of the indirect pathway of abscisic acid biosynthesis by mutants, genes, and enzymes. Plant Physiol **131,** 1591-1601.

Shumskaya, M., and Wurtzel, E.T. (2013). The carotenoid biosynthetic pathway: thinking in all dimensions. Plant Sci **208,** 58-63.

Story, E.N., Kopec, R.E., Schwartz, S.J., and Harris, G.K. (2010). An update on the health effects of tomato lycopene. Annu Rev Food Sci Technol **1,** 189-210.

Walley, J., Xiao, Y.M., Wang, J.Z., Baidoo, E.E., Keasling, J.D., Shen, Z.X., Briggs, S.P., and Dehesh, K. (2015). Plastid-produced interorgannellar stress signal MEcPP potentiates induction of the unfolded protein response in endoplasmic reticulum. P Natl Acad Sci USA **112,** 6212-6217.

Ye, X., Al-Babili, S., Kloti, A., Zhang, J., Lucca, P., Beyer, P., and Potrykus, I. (2000). Engineering the provitamin A (beta-carotene) biosynthetic pathway into (carotenoid-free) rice endosperm. Science **287,** 303-305.

Yu, Q.J., Ghisla, S., Hirschberg, J., Mann, V., and Beyer, P. (2011). Plant Carotene Cis-Trans Isomerase CRTISO a new member of the FAD(red)-dependent flavoproteins catalyzingbnon-redox reactions. J Biol Chem **286,** 8666-8676.

Zechmeister, L., Lerosen, A.L., Went, F.W., and Pauling, L. (1941). Prolycopene, a Naturally Occuring Stereoisomer of Lycopene. Proc Natl Acad Sci U S A **27,** 468-474.

Zhang, Y., Buteli, E., Alseekh, S., Tohge, T., Rallapalli, G., Luo, J., kawar, P.G., Hill, L., Santino, A., Fernie, A.R. and Martin, C. (2015). Multi-level engineering facilitates the production of phenyl propanoid compounds in tomato. Nat Communications, 6, 8635.

Zhou, X.J., Welsch, R., Yang, Y., Alvarez, D., Riediger, M., Yuan, H., Fish, T., Liu, J.P., Thannhauser, T.W., and Li, L. (2015). *Arabidopsis* OR proteins are the major posttranscriptional regulators of phytoene synthase in controlling carotenoid biosynthesis. P Natl Acad Sci USA **112,** 3558-3563.

TABLES

Table 1. Carotenoid and chlorophyll contents of leaf (A), mature green fruit (B) and ripe fruit (C) from wild type (AC), AC expressing *crtI* (AC:*crtI*), the tangerine background (t^{3183}) and a stable T2 generation t^{3183} plant expressing *crtI* (*t*:*crtI*). (C) also shows carotenoid content of ripe fruit from the *old gold crimson* background (og^c) and a representative homozygous T1 og^c plant expressing *crt*I (og^c:*crt*I).

A. Leaf tissue

Pigment	AC	AC:*crtI*	t^{3183}	*t*:*crtI*-9-11
Chlorophyll a (mg/g dw)	1.1 ± 0.1	**0.7 ± 0.02****	1.0 ± 0.02	0.9 ± 0.04
Chlorophyll b (mg/g dw)	1.2 ± 0.01	**0.9 ± 0.01*****	1.2 ± 0.02	1.1 ± 0.04
Total Chlorophyll (mg/g dw)	2.2 ± 0.1	**1.6 ± 0.03****	2.2 ± 0.04	1.9 ± 0.1
β-Carotene	624.6 ± 76.1	411.2 ± 35.1	514.5 ± 17.9	451.9 ± 33.3
Lutein	357.6 ± 7.0	**204.8 ± 3.6*****	379.0 ± 2.1	**184.2 ± 5.5*****
Neoxanthin	130.7 ± 1.9	**105.8 ± 2.2****	132.9 ± 1.9	**104.5 ± 4.8****
Violaxanthin	157.7 ± 3.3	**239.1 ± 1.3*****	162.9 ± 2.6	**280.1 ± 8.9*****
Total Carotenoids (mg/g dw)	1.3 ± 0.1	**1.0 ± 0.04***	1.2 ± 0.02	**1.0 ± 0.1***
Chlorophyll:Carotenoid	1.7 ± 0.1	1.7 ± 0.1	1.8 ± 0.01	**1.9 ± 0.01***

B. Mature green fruit

Pigment	AC	AC:*crtI*	t^{3183}	*t*:*crtI*-9-11
Chlorophyll a	56.4 ± 6.04	**14.1 ± 1.4****	60.8 ± 5.8	**8.7 ± 1.1*****
Chlorophyll b	49.8 ± 2.04	**30.6 ± 0.6****	43.9 ± 3.6	**10.7 ± 0.2*****
Total Chlorophyll	106.2 ± 8.0	**44.7 ± 1.4****	104.7 ± 9.4	**19.4 ± 1.2*****
15-cis phytoene	n/d	n/d	2.8 ± 0.3	**1.0 ± 0.03****
Lycopene	n/d	n/d	n/d	1.3 ± 0.1
γ-Carotene	n/d	n/d	n/d	1.6 ± 0.1
β-Carotene	10.3 ± 1.1	**5.6 ± 0.1***	20.6 ± 2.7	21.2 ± 1.0
Lutein	3.0 ± 0.2	**1.3 ± 0.2****	2.8 ± 0.4	2.7 ± 0.1
Neoxanthin	14.2 ± 0.6	11.5 ± 1.9	21.5 ± 1.7	**5.9 ± 0.5*****
Violaxanthin	2.3 ± 0.3	**1.0 ± 0.1***	6.1 ± 0.4	**1.5 ± 0.1*****
Total Carotenoid	29.8 ± 1.7	**19.3 ± 0.3***	53.7 ± 5.5	**33.5 ± 1.4***
Chlorophyll:Carotenoid	3.6 ± 0.1	**2.3 ± 0.04****	2.0 ± 0.04	**0.6 ± 0.02*****

C. Ripe fruit

Pigment	AC	AC:*crtI*	t^{3183}	*t*:*crtI*-9-11	og^{c}	og^{c}:*crtI*-20-7
Cis-phytoene	135.4 ± 27.4	**14.1 ± 2.7****	582.2 ± 55.4	**50.6 ± 3.3****	420.8 ± 93.9	**81.1 ± 3.4*****
All-*trans*-phytoene	13.4 ± 0.6	n/d	32.8 ± 3.0	**1.5 ± 0.1****	n/d	n/d
Total phytoene	144.3 ± 24.6	**14.1 ± 2.7****	615.0 ± 58.4	**51.5 ± 3.1****	420.8 ± 93.9	**81.1 ± 3.4*****
Cis-phytofluene	75.1 ± 5.5	n/d	300.1 ± 22.4	**1.8 ± 0.2*****	n/d	n/d
All-*trans*-phytofluene	146.0 ± 3.3	**2.8 ± 0.6*****	36.0 ± 6.7	29.1 ± 1.4	104.3 ± 39.2	**34.8 ± 1.8*****
Total phytofluene	224.0 ± 8.1	**2.8 ± 0.6****	336.0 ± 27.6	**30.9 ± 1.6****	104.3 ± 39.2	**34.8 ± 1.8*****
Cis-ζ-Carotene	34.1 ± 3.6	n/d	157.5 ± 7.0	**17.6 ± 1.3*****	n/d	n/d
Cis-Neurosporene	n/d	n/d	250.1 ± 8.7	n/d	n/d	n/d
Prolycopene	n/d	n/d	2.3 ± 0.2	**1.7 ± 0.1***	n/d	n/d
(mg/g dw)						
Cis-lycopene	n/d	n/d	13.5 ± 2.6	**2.7 ± 0.2****	n/d	n/d
All-*trans*-lycopene	816.4 ± 173.7	695.3 ± 66.5	13.5 ± 3.5	**52.9 ± 2.6*****	5695.6 ± 1090.3	5561.5 ± 292.0
Total lycopene	816.4 ± 173.7	695.3 ± 66.5	27.0 ± 6.1	**54.7 ± 3.7****	5695.6 ± 1090.3	5561.5 ± 292.0
β-Carotene	122.9 ± 17.0	**708.7 ± 36.9*****	n/d	**477.1 ± 20.9*****	166.5 ± 39.4	**392.6 ± 15.7*****

Lutein	25.5 ± 2.6	25.6 ± 4.3	8.3 ± 1.4	**12.6 ± 0.5***	61.8 ± 12.9	**71.9 ± 2.4***
Neoxanthin	n/d	**1.4 ± 0.1****	n/d	**6.1 ± 0.3*****	n/d	n/d
Violaxanthin	n/d	**5.3 ± 0.3***	n/d	**7.1 ± 0.4*****	n/d	n/d
Total carotenoid (mg/g dw)	1.30 ± 0.2	1.5 ± 0.1	3.7 ± 0.3	**2.4 ± 0.1*****	6.45 ± 1.58	6.14 ± 0.26

Carotenoid and chlorophyll contents are presented as μg/g dry weight (dw) unless otherwise stated in the table. Values are the mean of a minimum of 3 biological and 3 technical replicates ± standard deviation. Significant differences to the appropriate background are indicated in bold and were determined by Student's *t* tests. The P-Values are indicated as follows, 0.05 - *, 0.01 - **, 0.001 - ***

Table 2. Isoprenoid and carotenogenic enzyme activities determined in wild type tomato fruit and varieties with altered carotene desaturation/isomerisation.Enzyme	AC	AC:*crtI*	t^{3183}	*t*:*crtI*-9-11
DXS	774x10^3 ± 37	**517**x10^3 **± 14****	**1178**x10^3 **± 61****	**660**x10^3 **± 29*****
IPP isomerase	83x10^3 ± 1	**45**x10^3 **± 3****	105x10^3 ± 12	**49**x10^3 **± 12***
Geranylgeranyl PP synthase	296x10^3 ± 7	263x10^3 ± 12	**523**x10^3 **± 67***	317x10^3 ± 44
Phytoene synthase	12x10^3 ± 1	**9x10^3 ± 0.1***	16x10^3 ± 3	**8x10^3 ± 1***
Phytoene desaturase	0.75x10^3 ± 67	0.89x10^3 ± 66	**0.35x10^3 ± 31****	**0.60x10^3 ± 133****
Lycopene β-cyclase	0.26x10^3 ± 92	**1.12x10^3 ± 174****	**0.16x10^3 ± 59****	0.24x10^3 ± 76

Details of the assays are described in the Experimental Procedures. Enzyme activities are presented as dpm/mg prot./h. The stromal protein levels used for determining DXS, IPI, GGPPS and PSY were between 150 to 200 μg. Phytoene and lycopene desaturation and cyclisation respectively, were determined in the plastid membrane fraction and had a protein concentration of ~2 mg per ml. In the case of desaturation and cyclisation, the substrate generated *in situ* was 70 0000 and 50 000 dpm for phytoene and lycopene, respectively. Three independent

determinations were made. The data represents the average of three replicates ± SEM. Student *t*-tests were carried out to obtain an indication of the statistical significance. Those values showing a significant difference to the wild type (AC) are provided in bold and *, ** and *** indicates p values of 0.05, 0.05 and 0.0001 respectively.

Table 3. Metabolites in ripe fruit pericarp from AC expressing *crtI* (AC:*crtI*) relative to the wild type AC control, the tangerine background (t^{3183}) relative to the AC control, a stable T2 generation t^{3183} plant expressing *crtI* (*t*:*crtI*) relative to its background t^{3183} and relative to the AC control.

Compound	AC/AC:*crtI*	AC/t^{3183}	t^{3183}/ *t*:*crtI*-9-11	AC/ *t*:*crtI*-9-11
Phenylpropanoids				
5-Caffeoylquinic acid	**2.2 ± 0.2***	1.0 ± 0.1	**1.7 ± 0.1***	**1.7 ± 0.2***
Chlorogenic acid	**11.7 ± 1.4****	**5.0 ± 0.3****	**0.2 ± 0.03*****	1.10 ± 0.1
Isochlorogenic acid	100 ± 3.1 #	n/d ± n/d	n/d ± n/d	n/d ± n/d
Naringenin:chalcone	1.4 ± 0.2	0.7 ± 0.1	**4.7 ± 0.2****	**3.3 ± 0.1****
Rutin	**1.7 ± 0.1***	0.6 ± 0.04	**1.5 ± 0.1***	0.9 ± 0.03
Triterpenes				
β-Amyrin	**2.2 ± 0.2****	**0.2 ± 0.03*****	**5.6 ± 0.2*****	1.1 ± 0.04
Campesterol	**0.8 ± 0.04****	**0.6 ± 0.01*****	**1.7 ± 0.1****	1.0 ± 0.1
Cycloartenol	**1.9 ± 0.1*****	**0.5 ± 0.03*****	**3.1 ± 0.1*****	**1.5 ± 0.02*****

β-Sitosterol	1.3	±	0.2	1.1	±	0.03	1.2	±	0.1	1.2	±	0.1
Stigmasterol	**1.2**	±	**0.1***	**0.7**	±	**0.03*****	**2.0**	±	**0.1*****	**1.4**	±	**0.1****
Organic acids												
Aconitic acid	**0.8**	±	**0.04****	**1.8**	±	**0.3***	0.7	±	0.1	1.2	±	0.2
Ascorbic acid	**2.5**	±	**0.2****	1.4	±	0.1	1.1	±	0.3	1.6	±	0.4
Benzoic acid	1.0	±	0.1	**0.8**	±	**0.1***	1.0	±	0.04	**0.8**	±	**0.04****
Citric acid	**0.5**	±	**0.03*****	**1.4**	±	**0.01*****	**0.8**	±	**0.1***	1.1	±	0.1
Dehydroascorbic acid	**2.1**	±	**0.2****	1.0	±	0.3	1.4	±	0.1	**1.4**	±	**0.1****
Fumaric acid	**1.4**	±	**0.1***	**2.1**	±	**0.4***	1.4	±	0.2	**2.8**	±	**0.5***
Lactic acid	0.8	±	0.1	0.7	±	0.1	1.2	±	0.1	0.9	±	0.1
Galactonic acid	**0.6**	±	**0.03*****	**0.6**	±	**0.01*****	1.0	±	0.04	**0.6**	±	**0.03*****
Galacturonic acid	**0.3**	±	**0.03*****	**0.5**	±	**0.002*****	0.9	±	0.1	**0.5**	±	**0.03*****
Gluconic acid	1.4	±	0.3	2.0	±	0.2	0.9	±	0.1	1.8	±	0.2
Glyceric acid	**2.3**	±	**0.04*****	0.8	±	0.1	**2.0**	±	**0.01*****	**1.6**	±	**0.01*****
Glycolic acid	**1.7**	±	**0.1***	1.1	±	0.1	1.1	±	0.01	1.2	±	0.01
Malic acid	1.1	±	0.04	**2.1**	±	**0.1*****	1.2	±	0.1	**2.6**	±	**0.2****
2-Oxoglutaric acid	1.2	±	0.1	1.0	±	0.04	0.9	±	0.02	0.9	±	0.02
Quinic acid	**0.9**	±	**0.03***	**0.8**	±	**0.03****	0.8	±	0.1	**0.7**	±	**0.1****
Succinic acid	**1.9**	±	**0.1****	0.9	±	0.03	1.2	±	0.1	1.0	±	0.1

Amino acids												
Alanine	1.0	±	0.03	**0.9**	±	**0.01****	**0.6**	±	**0.04*****	**0.6**	±	**0.03*****
β-Alanine	0.4	±	0.02	0.7	±	0.03	**0.7**	±	**0.1****	0.5	±	0.04
4-aminobutryic acid	**0.4**	±	**0.01*****	**0.8**	±	**0.01*****	**0.8**	±	**0.1***	**0.6**	±	**0.04*****
Asparagine	**1.3**	±	**0.1***	**1.8**	±	**0.04*****	**0.8**	±	**0.03****	**1.4**	±	**0.1****
Aspartic acid	**0.9**	±	**0.04***	**1.4**	±	**0.003*****	**0.4**	±	**0.02*****	**0.6**	±	**0.03*****
Cysteine	**5.4**	±	**0.3*****	**5.9**	±	**0.3*****	0.8	±	0.1	**4.5**	±	**0.5****
Glutamic acid	**0.5**	±	**0.02*****	**1.3**	±	**0.01*****	**0.3**	±	**0.02*****	**0.4**	±	**0.02*****
Glutamine	**1.3**	±	**0.1****	**1.9**	±	**0.1*****	**0.5**	±	**0.04****	1.0	±	0.1
Glycine	**0.4**	±	**0.02*****	**0.6**	±	**0.01*****	1.0	±	0.1	**0.6**	±	**0.04****
Leucine	0.9	±	0.1	**0.9**	±	**0.01***	**0.6**	±	**0.02*****	**0.5**	±	**0.02*****
Lysine	0.9	±	0.1	0.9	±	0.1	0.9	±	0.1	**0.8**	±	**0.04****
5-Oxo-proline	1.0	±	0.1	**1.3**	±	**0.1***	**0.5**	±	**0.04****	**0.6**	±	**0.1****
Serine	**0.8**	±	**0.04****	**1.5**	±	**0.03*****	**0.5**	±	**0.02*****	**0.8**	±	**0.03****
Threonine	**0.9**	±	**0.03***	**1.2**	±	**0.03****	**0.7**	±	**0.04****	**0.8**	±	**0.1***
Valine	**0.8**	±	**0.03****	**0.9**	±	**0.03****	**0.8**	±	**0.1***	**0.7**	±	**0.04*****
Fatty acids												
Linoleic acid	0.7	±	0.2	**0.6**	±	**0.1***	0.9	±	0.1	**0.5**	±	**0.1***
Palmitic acid	1.1	±	0.03	0.8	±	0.1	1.0	±	0.1	**0.8**	±	**0.1*****
Stearic acid	0.9	±	0.1	0.8	±	0.1	0.7	±	0.1	**0.5**	±	**0.1****

Sugars											
Arabinose	1.8	±	0.04	0.6	±	0.03	**1.2**	±	**0.02***	0.8	± 0.01
Fructose	**0.9**	±	**0.03****	1.0	±	0.1	0.9	±	0.1	0.9	± 0.1
Gentiobiose	1.5	±	0.2	0.9	±	0.1	1.1	±	0.1	1.0	± 0.1
Glucose	**0.8**	±	**0.01*****	0.9	±	0.1	0.9	±	0.1	**0.8**	± **0.04****
Maltose	**1.9**	±	**0.02****	0.8	±	0.04	0.7	±	0.04	**0.6**	± **0.03***
Melizitose	**0.1**	±	**0.1****	**0.5**	±	**0.02****	**0.2**	±	**0.1****	**0.1**	± **0.1*****
Rhamnose	**3.3**	±	**0.2****	1.0	±	0.03	**1.9**	±	**0.2***	**1.8**	± **0.2***
Ribose	1.0	±	0.03	0.9	±	0.4	0.8	±	0.1	0.7	± 0.1
Sedoheptulose	**8.6**	±	**1.4****	1.1	±	0.02	**3.9**	±	**0.1*****	**4.4**	± **0.1*****
Sucrose	**3.1**	±	**0.2*****	**0.2**	±	**0.04*****	**5.9**	±	**0.6****	0.9	± 0.1
Xylose	**1.3**	±	**0.1***	**0.8**	±	**0.01****	1.2	±	0.1	1.0	± 0.1
Polyols											
Glycerol	**0.7**	±	**0.1***	**0.8**	±	**0.03****	**0.8**	±	**0.1***	**0.6**	± **0.04****
Inositol	**0.6**	±	**0.02*****	**0.6**	±	**0.01*****	**0.5**	±	**0.03*****	**0.3**	± **0.02*****
Mannitol	**2.5**	±	**0.3***	1.2	±	0.3	1.0	±	0.1	1.2	± 0.1
Phosphates											
Fructose-6-phosphate	**1.6**	±	**0.1****	**1.3**	±	**0.1***	0.9	±	0.1	1.1	± 0.1

Glucose-6-phosphate	**1.6**	±	**0.2***	1.2	±	0.1	1.0	±	0.02	**1.2**	±	**0.02****
Glycerol-3-phosphate	1.1	±	0.1	**1.4**	±	**0.1***	**0.6**	±	**0.1***	**0.8**	±	**0.1***
Inositol-6-phosphate	**0.6**	±	**0.1***	**0.4**	±	**0.1****	1.4	±	0.2	**0.6**	±	**0.1***
Phosphate	**0.9**	±	**0.04***	1.0	±	0.03	0.9	±	0.04	1.0	±	0.04
Sorbitol-6-phosphate	1.0	±	0.1	**0.7**	±	**0.01***	1.3	±	0.2	0.9	±	0.1
***N*-Containing Compounds**												
Putrescine	**1.2**	±	**0.03***	**0.7**	±	**0.01*****	**2.4**	±	**0.2****	**1.6**	±	**0.1***

Values are the mean of a minimum of 3 biological and 3 technical replicates ± standard deviation. Significant differences are indicated in bold and were determined by Student's *t* tests. The P-Values are indicated as follows, 0.05 - *, 0.01 - **, 0.001 - ***.

FIGURE LEGENDS

Figure 1. Carotenoid biosynthesis highlighting the difference in desaturation found in plants/algae and fungi/bacteria.

In fungi and bacteria, the 15-*cis*-phytoene undergoes a series of four sequential desaturation steps and one isomerisation at the C15-C15´ double bond to yield lycopene via phytofluene, ζ-carotene and neurosporene with all steps catalysed by a single enzyme, phytoene desaturase/isomerase (crtI). In plants, algae and also cyanobacteria, phytoene desaturase (PDS) carries out the first two desaturation steps to yield 9,15,9´-tri-*cis*-ζ-carotene. The central double bond is then isomerised by ZISO to generate 9,9´-di-*cis*-ζ-carotene, the further desaturation of which is catalysed by ζ-Carotene desaturase (ZDS). This results in the introduction of two further cis bonds in the 7 and 7´ positions to yield 7,9,7´,9´-tetra-*cis*-lycopene via 7,9,9´-tri-*cis*-neurosporene which are isomerised to the all-*trans* form of lycopene by CRTISO. Black arrows indicate the positions where double bonds are introduced, red arrows and numbering indicate the position of the *cis* bonds.

Figure 2. Carotenoid pathway gene expression profiles of Ailsa Craig and *tangerine*, with and without *crtI* expressed, relative to the wild type Ailsa Craig background, in 3 days post breaker fruit.

Total RNA was extracted from pooled 3 days post breaker fruit originating from 3 plants per line. qRT-PCR was performed with gene-specific primers for (1) *DXS*, 1-deoxy-D-xylulose-5-phosphate synthase; (2) *GGPPS1*, geranylgeranyl pyrophosphate synthase-1; (3) *GGPPS2*, geranylgeranyl pyrophosphate synthase-2; (4) *PSY1*, phytoene synthase-1; (5) *PSY2*, phytoene synthase-2; (6) *PDS*, phytoene desaturase; (7) *ZDS*, ζ-carotene desaturase; (8)

CRTISO, carotene isomerise; (9) *crtI*, bacterial phytoene desaturase; (10) *LCYB*, β-lycopene cyclase; (11) *CYCB*, lycopene cyclase B; (12) *LCYE*, ε-lycopene cyclase. Expression data was normalised to the expression level of actin. AC, Ailsa Craig wild type control; AC:*crtI*, *crtI* expressed in the AC background; t^{3183}, tangerine background; *t*:*crtI*-9-11, *crtI* expressed in the tangerine background. Statistical determinations are shown as mean ± standard deviation, where n=3 to 6. The P-Values, as determined by one-way ANOVA, are indicated as follows, 0.05 - *, 0.01 - **, 0.001 - ***.

Figure 3. Carotenoid pathway gene expression profile of og^c with and without *crtI* expressed relative to the wild type AC, in 3 days post breaker fruit.

Total RNA was extracted from pooled 3 days post breaker fruit originating from 3 plants per line. qRT-PCR was performed with gene-specific primers for (1) *DXS*, 1-deoxy-D-xylulose-5-phosphate synthase; (2) *GGPPS1*, geranylgeranyl pyrophosphate synthase-1; (3) *GGPPS2*, geranylgeranyl-l pyrophosphate synthase-2; (4) *PSY1*, phytoene synthase-1; (5) *PSY2*, phytoene synthase-2; (6) *PDS*, phytoene desaturase; (7) *ZDS*, ζ-carotene desaturase; (8) *CRTISO*, carotene isomerise; (9) *crtI*, bacterial phytoene desaturase; (10) *LCYB*, β-lycopene cyclase; (11) *CYCB*, lycopene cyclase B; (12) *LCYE*, ε-lycopene cyclase. Expression data was normalised to the expression level of actin. AC, Ailsa Craig control; og^c, old gold crimson; og^c:*crtI-22-6*, *crtI* expressed in the og^c background. Statistical determinations are shown as mean ± standard deviation, where n=3 to 6. The P-Values, as determined by one-way ANOVA, are indicated as follows, 0.05 - *, 0.01 - **, 0.001 - ***.

Figure 4. Schematic representation summarising the differential expression of β-lycopene cyclase (*LCYB*) and *CYCB* transcripts in response to the effects mediated by the presence of crtI in different genotypes.

(A) Shows an increase in *LCYB* transcripts (>2-fold) as indicated by the thickness of the arrow, in response to the presence of crtI in a wild type Ailsa Craig, (AC), background. This change in transcript levels is accompanied by a 2 to 4-fold increase in β-carotene as represented by the shading. The lycopene and levels of *CYCB* transcripts were unchanged. (B) Illustrates the comparison between perturbed cyclase(s) expression in the t^{3183} genotype and the *t:crtI* genotype. Both the lycopene and β-carotene contents (<15 mg/g dw or undetectable in t^{3183} respectively) were significantly increased; lycopene >4-fold the t^{3183} level and β-carotene >3.5-fold the AC level. These changes in metabolites, indicated by the shading, correlated with increased *CYCB* solely, the expression of *LCYB* was unaffected. (C) In the Og^{c} background the *CYCB* is null as indicated by the dashed arrows and horizontal double lines. In this case, the *LCYB* transcripts are up-regulated (2 to 4-fold; as shown by the thickness of the arrows) and although lycopene does not increase, β-carotene levels are elevated 4 to 6-fold as indicated by the shading.

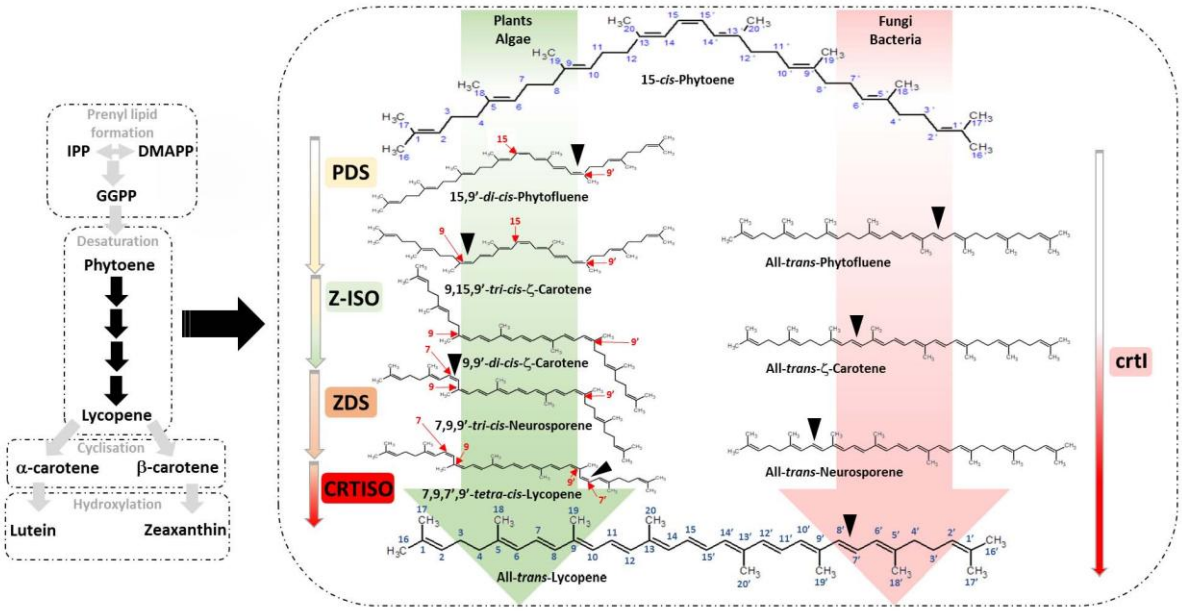

Figure 1. Carotenoid biosynthesis highlighting the difference in desaturation found in plants/algae and fungi/bacteria. In fungi and bacteria, the 15-*cis*-phytoene undergoes a series of four sequential desaturation steps and one isomerisation at the C15-C15′ double bond to yield lycopene via phytofluene, ζ-carotene and neurosporene with all steps catalysed by a single enzyme, phytoene desaturase/isomerase (crtI). In plants, algae and also cyanobacteria, phytoene desaturase (PDS) carries out the first two desaturation steps to yield 9,15,9′-tri-*cis*-ζ-carotene. The central double bond is then isomerised by ZISO to generate 9,9′-di-*cis*-ζ-carotene, the further desaturation of which is catalysed by ζ-Carotene desaturase (ZDS). This results in the introduction of two further cis bonds in the 7 and 7′ positions to yield 7,9,7′,9′-tetra-*cis*-lycopene via 7,9,9′-tri-*cis*-neurosporene which are isomerised to the all-*trans* form of lycopene by CRTISO. Black arrows indicate the positions where double bonds are introduced, red arrows and numbering indicate the position of the *cis* bonds.

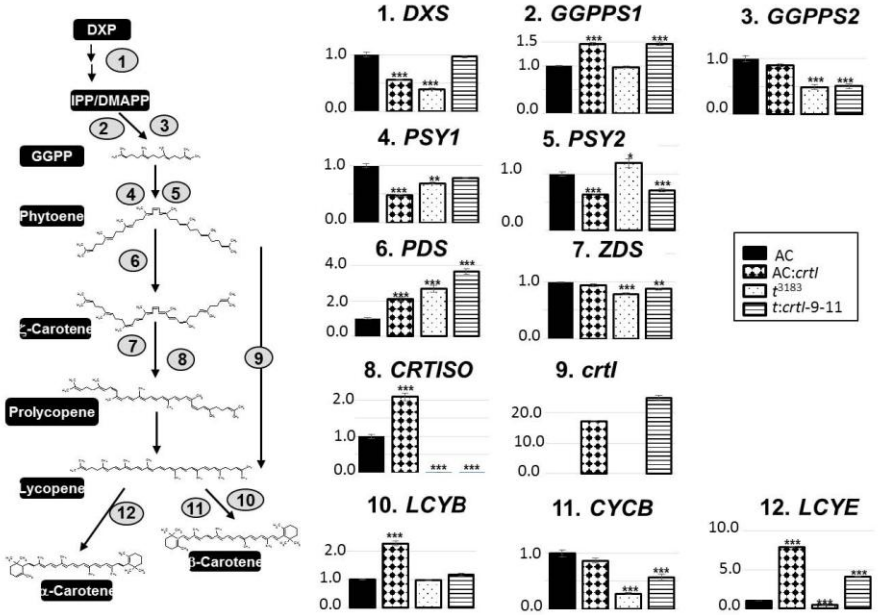

Figure 2. Carotenoid pathway gene expression profiles of Ailsa Craig and *tangerine*, with and without *crtI* expressed, relative to the wild type Ailsa Craig background, in 3 days post breaker fruit. Total RNA was extracted from pooled 3 days post breaker fruit originating from 3 plants per line. qRT-PCR was performed with gene-specific primers for (1) *DXS*, 1-deoxy-D-xylulose-5-phosphate synthase; (2) *GGPPS1*, geranylgeranyl pyrophosphate synthase-1; (3) *GGPPS2*, geranylgeranyl pyrophosphate synthase-2; (4) *PSY1*, phytoene synthase-1; (5) *PSY2*, phytoene synthase-2; (6) *PDS*, phytoene desaturase; (7) *ZDS*, ζ-carotene desaturase; (8) *CRTISO*, carotene isomerise; (9) *crtI*, bacterial phytoene desaturase; (10) *LCYB*, β-lycopene cyclase; (11) *CYCB*, lycopene cyclase B; (12) *LCYE*, ε-lycopene cyclase. Expression data was normalised to the expression level of actin. AC, Ailsa Craig wild type control; AC:*crtI*, *crtI* expressed in the AC background; t^{3183}, tangerine background; *t*:*crtI*-9-11, *crtI* expressed in the tangerine background. Statistical determinations are shown as mean ± standard deviation, where n=3 to 6. The P-Values, as determined by one-way ANOVA, are indicated as follows, 0.05 - *, 0.01 - **, 0.001 - ***.

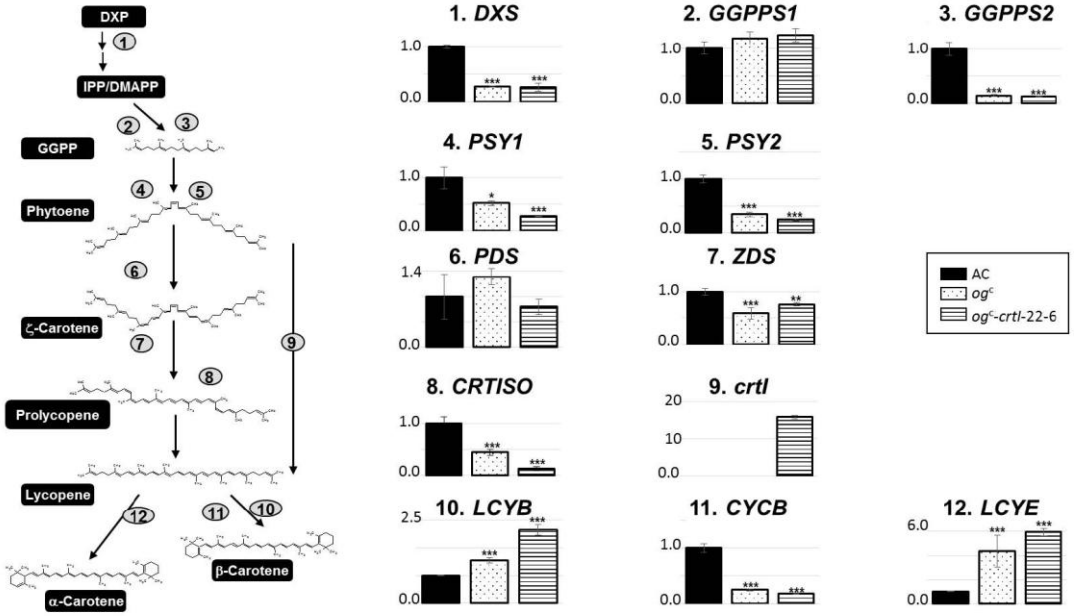

Figure 3. Carotenoid pathway gene expression profile of og^c with and without *crtI* expressed relative to the wild type AC, in 3 days post breaker fruit. Total RNA was extracted from pooled 3 days post breaker fruit originating from 3 plants per line. qRT-PCR was performed with gene-specific primers for (1) *DXS*, 1-deoxy-D-xylulose-5-phosphate synthase; (2) *GGPPS1*, geranylgeranyl pyrophosphate synthase-1; (3) *GGPPS2*, geranylgeranyl-l pyrophosphate synthase-2; (4) *PSY1*, phytoene synthase-1; (5) *PSY2*, phytoene synthase-2; (6) *PDS*, phytoene desaturase; (7) *ZDS*, ζ-carotene desaturase; (8) *CRTISO*, carotene isomerise; (9) *crtI*, bacterial phytoene desaturase; (10) *LCYB*, β-lycopene cyclase; (11) *CYCB*, lycopene cyclase B; (12) *LCYE*, ε-lycopene cyclase. Expression data was normalised to the expression level of actin. AC, Ailsa Craig control; og^c, old gold crimson; og^c*:crtI-22-6*, *crtI* expressed in the og^c background. Statistical determinations are shown as mean ± standard deviation, where n=3 to 6. The P-Values, as determined by one-way ANOVA, are indicated as follows, 0.05 - *, 0.01 - **, 0.001 - ***.

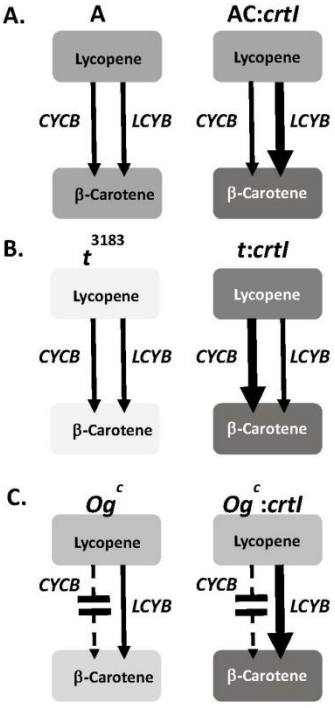

Figure 4. Schematic representation summarising the differential expression of β-lycopene cyclase (*LCYB*) and *CYCB* transcripts in response to the effects mediated by the presence of crtI in different genotypes.

A. Shows an increase in *LCYB* transcripts (>2-fold) as indicated by the thickness of the arrow, in response to the presence of crtI in a wild type Ailsa Craig, (AC), background. This change in transcript levels is accompanied by a 2 to 4-fold increase in β-carotene as represented by the shading. The lycopene and levels of *CYCB* transcripts were unchanged.

B. Illustrates the comparison between perturbed cyclase(s) expression in the t^{3183} genotype and the *t:crtI* genotype. Both the lycopene and β-carotene contents (<15 µg/g dw or undetectable in t^{3183} respectively) were significantly increased; lycopene >4-fold the t^{3183} level and β-carotene >3.5-fold the AC level. These changes in metabolites, indicated by the shading, correlated with increased *CYCB* solely, the expression of *LCYB* was unaffected.

C. In the Og^c background the *CYCB* is null as indicated by the dashed arrows and horizontal double lines. In this case the *LCYB* transcripts are up-regulated (2 to 4-fold; as shown by the thickness of the arrows) and although lycopene does not increase, β-carotene levels are elevated 4 to 6-fold as indicated by the shading.